

# Estimating Chlorophyll-a Concentrations in Indian River Lagoon, FL

Final Report

By:

Hannes Ziegler

For:

GIS 6127C Hyperspectral Remote Sensing

Dr. Cayan Zhang

Graduate Final

5/2/2016

## Introduction

The concentrations of chlorophyll-a (chl-a) in the environmentally stressed Indian River Lagoon (IRL), FL are estimated and mapped using remotely sensed hyperspectral data. To accomplish this, the spectral characteristics of chl-a constituents in estuarine waters are used to calibrate a model against in-situ measurements of chl-a concentrations. The model is then used to extrapolate estimated chl-a concentrations across the imagery on a cell-by-cell basis, producing a continuous mapped surface. Spectral data is obtained from atmospherically corrected and georeferenced imagery from HICO, the Hyperspectral Imager for the Coastal Ocean, while in-situ measurements are obtained from the St. Johns River Water Management District (SJRWMD).

The IRL is a lagoon system that stretches 156 miles from Jupiter to Ponce inlet along the east coast of Florida (Lapointe, Herren, Debortoli, & Vogel, 2015) Originally a thriving ecosystem, the lagoon has experienced substantial degradation due to the creation of drainage canals, agriculture, urban expansion, and mosquito control (Lapointe, Herren, Debortoli, & Vogel, 2015) Anthropogenic influences have enriched IRL waters with nutrients, leading to algae blooms such as the superbloom of 2011 (Kamerosky, Cho, & Morris, 2015; Lapointe, Herren, Debortoli, & Vogel, 2015). These have in turn resulted in a decline in seagrass and wildlife (Lapointe, Herren, Debortoli, & Vogel, 2015). Commercial and recreational activities that rely on the health of IRL had an estimated value of \$3.4 billion in 2007 (Lapointe, Herren, Debortoli, & Vogel, 2015). This means the preservation of the IRL's health is important not just for wild flora and fauna, but also for the local residents, tourists, and industries. Therefore, monitoring algae concentrations in the IRL are an important activity in support of environmental management and preservation.

## Problem Statement and Objectives

While in-situ point measurements regularly obtained by SJRWMD provide a good basis for understanding the water quality of IRL, they are disperse and discrete, and cannot by themselves deliver a complete picture. However, it would hardly be practical or efficient to obtain in-situ measurements for every point within IRL. Recent research, however, has suggested that the remotely sensed spectral characteristics of water can be used to map chl-a and other water constituent concentrations on a system-wide scale (Kamerosky, Cho, & Morris, 2015; Bhatti, Schalles, Rundquist, Ramirez, & Nasu, 2010; Gitelson, Gao, Li, Berdnikov, & Saprygin, 2011; Olmanson, Brezonik, & Bauer, 2013; Shafique, Fulk, Autrey, & Flotemersch, 2003; Spectral Imaging Ltd.). The objective is thus to 1) optimize the wavelengths used to distinguish chl-a constituents in water, 2) to calibrate a model with the in-situ measurements of chl-a, and 3) to use the model to map chl-a concentrations across the obtained imagery. The optimized model's performance will be compared with a model transferred from the Azov Sea in Russia, and a model based on visual inspection of spectral profiles alone.

It is expected that the optimized model will perform best, and that transferring models calibrated to other water bodies (in this case the Azov Sea) is unreliable. It is also expected that waters close to areas with anthropogenic influence (i.e. towns, industrial sites, canals) will exhibit elevated chl-a concentrations due to sources of eutrophication.

## Literature Review

Hyperspectral remote sensing has shown itself to be effective in mapping chl-a concentrations in turbid inland (Bhatti, Schalles, Rundquist, Ramirez, & Nasu, 2010; Shafique,

Fulk, Autrey, & Flotemersch, 2003; Spectral Imaging Ltd.) and estuarine or coastal case-II waters (Gitelson, Gao, Li, Berdnikov, & Saprygin, 2011; Bhatti, Schalles, Rundquist, Ramirez, & Nasu, 2010). Case-II waters such as IRL (Kamerosky, Cho, & Morris, 2015) contain multiple constituents, making multispectral imagery with fewer bands than hyperspectral imagery less ideal (Bhatti, Schalles, Rundquist, Ramirez, & Nasu, 2010).

Mapping of chl-a using hyperspectral imagery involves taking in-situ samples from the target water body and using these samples to calibrate a model which can then be used to map chl-a concentrations throughout the water body with hyperspectral imagery. The methodology used by these studies is based on the spectral signal of turbid waters that contain chl-a as a constituent. The spectral signatures of such waters exhibit a strong electromagnetic wavelength absorption around 450-475nm, maximum reflectance at 550nm, strong absorption around 670nm, and a reflectance peak near the 700nm (Bhatti, Schalles, Rundquist, Ramirez, & Nasu, 2010; Gitelson, Gao, Li, Berdnikov, & Saprygin, 2011; Olmanson, Brezonik, & Bauer, 2013). Models are calibrated to the target water body (lake, estuary, river, etc.) based upon the strength of the regression between chl-a concentration and an equation that characterizes the spectral responses of select bands to chl-a. Usually, the ratios of two bands are used, generally one near 700nm and one near 670m (Bhatti, Schalles, Rundquist, Ramirez, & Nasu, 2010; Shafique, Fulk, Autrey, & Flotemersch, 2003), but three bands can also be used with the near-infrared band used to correct for surface reflectance (Gitelson, Gao, Li, Berdnikov, & Saprygin, 2011).

Gitelson et. al (2011) use such a three-band model to map chl-a concentration over case-II waters in the Azov Sea in Russia. They adapt an optimization procedure to minimize the root mean square error (RMSE) and find the optimal band wavelengths for measuring Chl-a are at  $\lambda_1 = 684\text{nm}$ ,  $\lambda_2 = 700\text{nm}$ , and  $\lambda_3 = 720\text{nm}$ . The reflectance values of those band wavelengths

(indicated by  $R\lambda_i$  where  $i$  is the associated wavelength) are then related to chl-a concentrations in the water using a regression where in-situ measurements of chl-a are the dependent variable and values obtained by calculating Equation 1 for the same location are the independent variable.

*Equation 1*

$$chl_a \propto \left( \frac{R\lambda_3}{R\lambda_1} - \frac{R\lambda_3}{R\lambda_2} \right)$$

The derived model explained more than 85% of the chl-a variation and allows estimation ranging between 17 and 93.14mg per cubic meter. The strong relationships found between bands and chl-a suggest great potential of hyperspectral data for monitoring chl-a concentrations in coastal and inland waters, and in this study these methods will be extended to IRL.

These methods require both in-situ measurements and hyperspectral imagery to temporally overlap, and the imagery also needs to be geometrically correct for spatial overlap of the data (Gitelson, Gao, Li, Berdnikov, & Saprygin, 2011; Olmanson, Brezonik, & Bauer, 2013). Furthermore, the imagery should be atmospherically corrected (Gitelson, Gao, Li, Berdnikov, & Saprygin, 2011; Olmanson, Brezonik, & Bauer, 2013), although it is noteworthy that good results have been obtained without atmospheric correction using multispectral imagery (Kamerosky, Cho, & Morris, 2015).

## Data & Data Processing

The hyperspectral imagery used in this study was obtained from the HICO spaceborne platform. HICO, which produced imagery until September 2014, has a spectral resolution of 87 bands from 380-960nm (Oregon State University, 2009). The spatial resolution varies due to changes of altitude and angle but is cited at 90m (Oregon State University, 2009). The platform was specifically designed for sampling of the coastal ocean and provides one 50x200km scene

per orbit (Oregon State University, 2009). The scene of IRL collected for this project was flown on February 28, 2014. This particular scene of IRL was not atmospherically corrected, and ENVI based FLAASH proved to be incapable of atmospherically correcting the imagery after several attempts (confirmed by contacting HICO operators). However, HICO operators at Oregon State University supply atmospherically corrected scenes by request. The scene of IRL used in this research was corrected by HICO operators with a version of Tafkaa\_6s (Atmospheric Correction for the Land) modified to include water vapor correction at 825nm to improve retrievals over coastal waters (Oregon State University, 2009). The attained imagery was not georeferenced and ArcMap supplied base-data at 0.3m resolution was used for rectification. The final processed imagery has a pixel dimensions of 88x88m.

In-situ water measurements of chl-a were obtained from St. Johns River Water Management District's (SJRWMD) Environmental Data Retrieval Tool. SJRWMD maintains a water quality monitoring network. Few stations are sampled on a monthly basis however, most stations are sampled once every other month for a variety of constituents, including chl-a in the units of  $\text{mg}/\text{m}^3$  (St. Johns River Water Management District, 2016). No measurements were taken on 2/28/2014, the acquisition date of the HICO imagery. In-situ measurement data was thus acquired within the date range 2/24/2014 – 3/5/2014 and the average chl-a concentration was calculated for each station. Gauge station coordinates were obtained by contacting the webmaster, and these were used to display the data in ArcGIS and extract reflectance values for use in modeling. Out of a total of 32 unique stations, only 10 fell within the study area and were located far enough from land and man-made structures to avoid spectral contamination of pixels sampled from the HICO imagery.

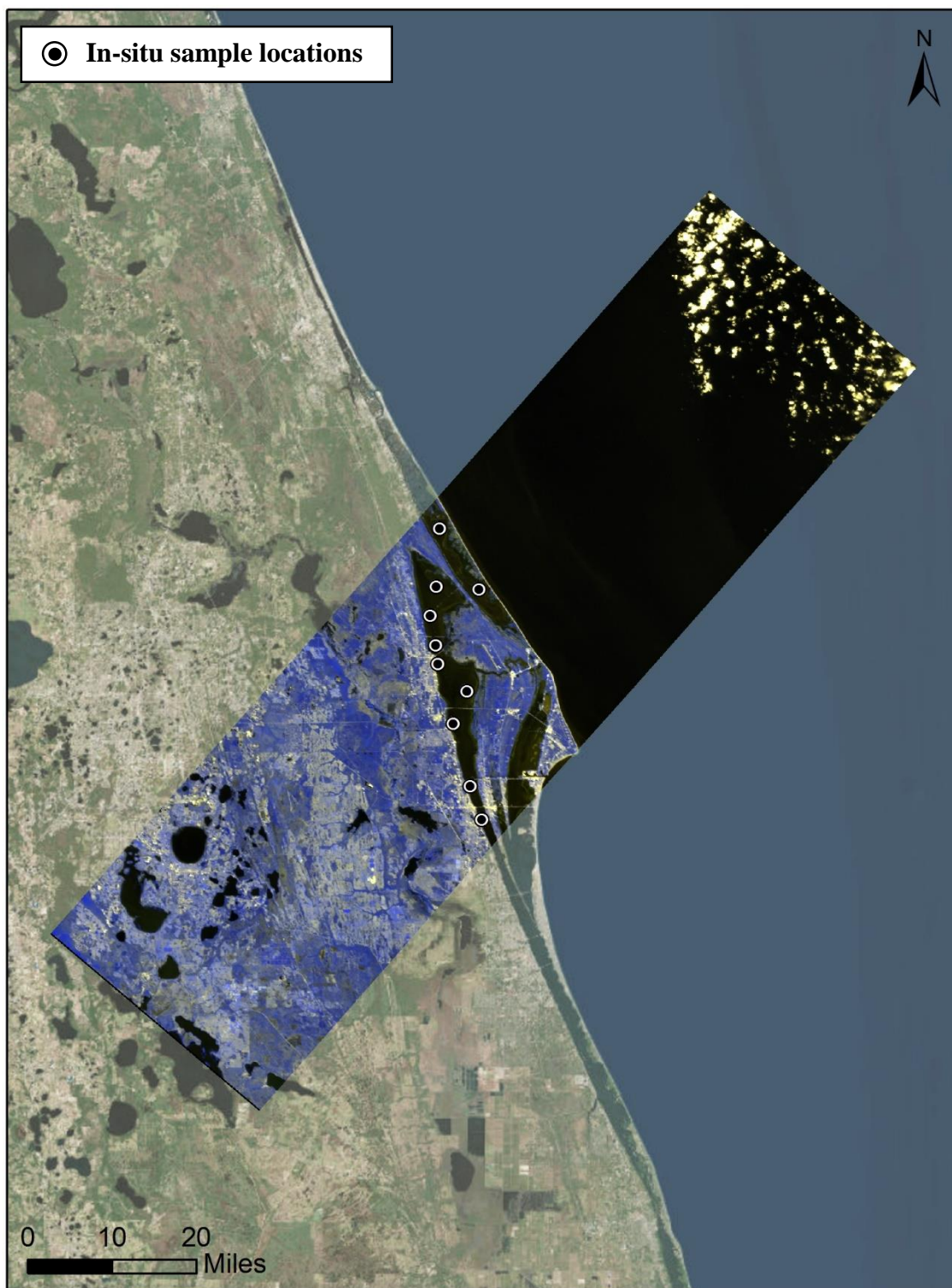


Figure 1: Atmospherically Corrected and Georeferenced HICO Imagery overlaid by the locations of gauge stations providing the in-situ chl-a measurements. HICO imagery obtained from Oregon State University, chl-a measurements obtained from St. Johns River Water Management District. Service layer credits: Esri, DigitalGlobe, GeoEye, Earthstar, Geographics, CNES/Airbus DS, USDA, USGS, AEX, Getmapping, Aerogrid, IGN, IGP, Swisstopo, and the GIS User Community.

## Methods & Analysis

A preliminary analysis of spectral profiles from IRL sampled in ENVI software confirmed the existence of the signature reflectance peak near 700nm and strong absorption near 670nm (Figure 2). Three models based on Equation 1 are calibrated to the in-situ measurements of chl-a via regression. Here, the dependent variable is the in-situ observed chl-a concentration ( $\text{mg}/\text{m}^3$ ), and the independent variable is the result of Equation 1 using the reflectance values extracted from the locations of in-situ measurements. The first model tested, model 1, uses the wavelengths suggested by Gitelson et. al (2011) in their study of the Azov Sea, Russia. As mentioned earlier, the model by Gitelson et al. (2011) found the optimal wavelengths to use lie at  $\lambda_1 = 684\text{nm}$ ,  $\lambda_2 = 700\text{nm}$ , and  $\lambda_3 = 720\text{nm}$ . Contrary to this, it is observed in spectral profiles of IRL that the actual peak appears to lie in this case at  $\lambda_2 = 690\text{nm}$ , with the absorption features at  $\lambda_1 = 678\text{nm}$  and  $\lambda_3 = 740\text{nm}$ . These values are used in model 2.

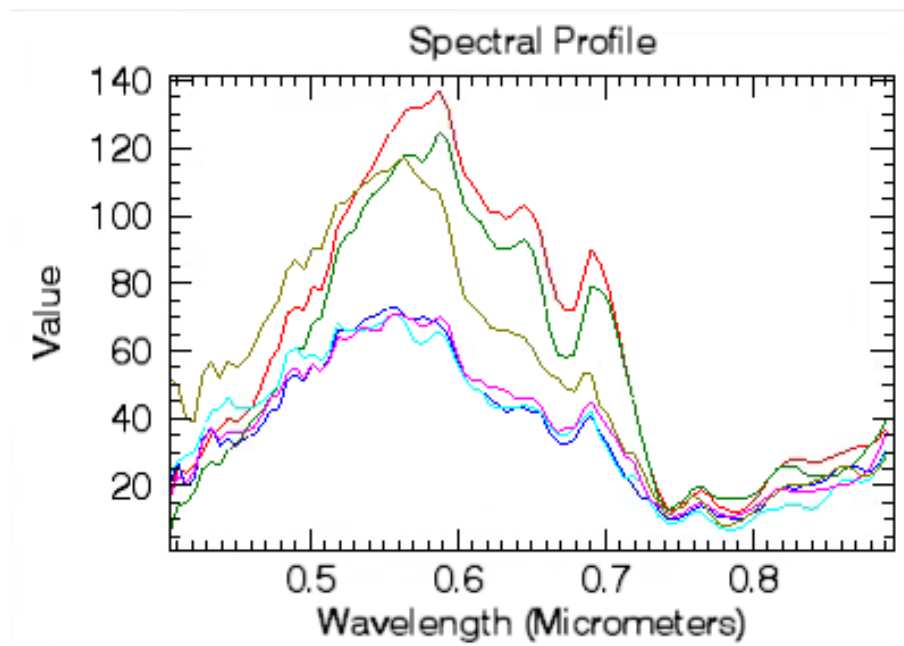


Figure 2: Sample of spectral profiles from IRL waters showing the characteristic peak near 700nm associated with chl-a in estuarine waters.



Model 3 makes use of an optimization procedure to identify the optimal wavelengths to use in the model, following methods similar to Gitelson et al. (2011). The optimization procedure works by choosing initial values of  $\lambda_1$  and  $\lambda_3$  and then regressing the results of Equation 1 against in-situ chl-a measurements using reflectance values at various wavelengths for  $\lambda_2$ . The optimal wavelength for  $\lambda_2$  is identified by observing the minimum RMSE. Once  $\lambda_2$  is fixed, the procedure is repeated once for  $\lambda_1$  and then for  $\lambda_3$ . This procedure was implemented in

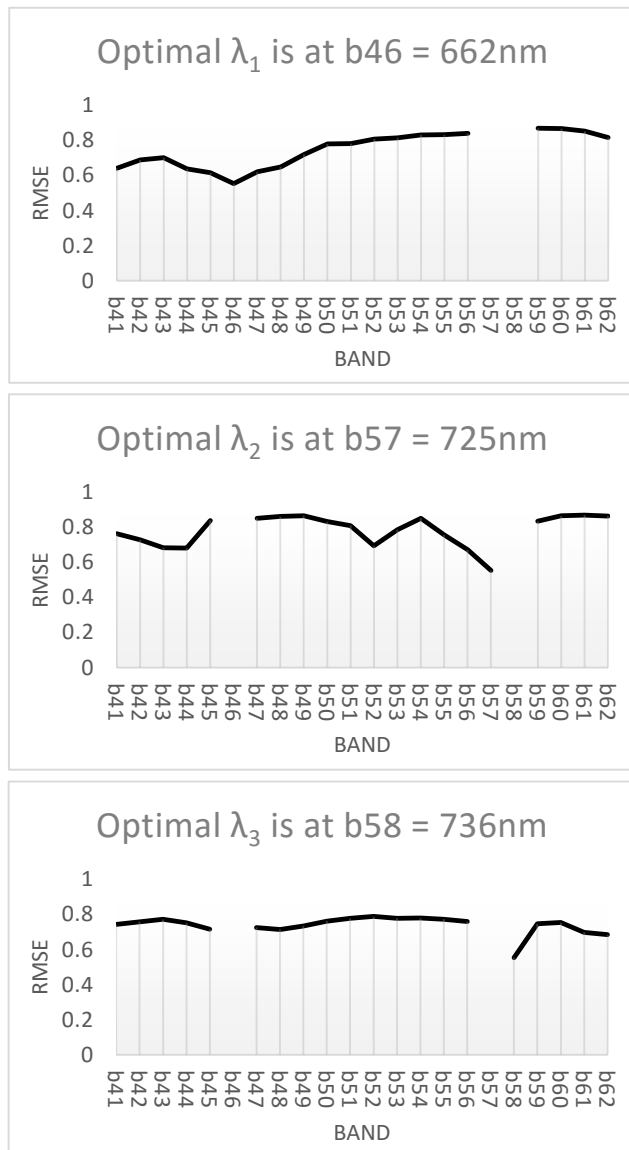


Figure 3: Optimal wavelengths to use  $\lambda_1$ ,  $\lambda_2$ , and  $\lambda_3$ , indicated by the smallest graphed RMSE values. Breaks in the line are due to fixed band values used during the optimization procedure.

Excel, and the developed Excel spreadsheet is versatile enough to be applicable to other projects where similar optimization might apply.

Based on the literature, the best wavelengths for modeling chl-a appear to be between 630nm and 750nm (Bhatti, Schalles, Rundquist, Ramirez, & Nasu, 2010; Gitelson, Gao, Li, Berdnikov, & Saprygin, 2011; Olmanson, Brezonik, & Bauer, 2013), and the optimization procedure was limited to these bands. For model 3, I thus obtained the optimal wavelengths  $\lambda_1 = 662$  nm,  $\lambda_2 = 725$ nm, and  $\lambda_3 = 736$ nm.

The resulting models are evaluated based upon the coefficient of determination ( $r^2$ ), ANOVA significance tests of the

regression, RMSE, and the coefficient of variation (CV). Only the best performing model is then mapped. The mapping procedure is implemented in ArcGIS by applying the model using the raster calculator tool, with a mask specifying the calculations to operate only on raster cells within IRL. Because the calibrated models may result in negative estimates of chl-a, and since the interpretation of these is impractical (there are no negative chl-a concentrations in the real world), any estimated chl-a values below zero are forced to equal zero.

## Results & Discussion

Out of the three models tested, model 3 with optimized wavelengths performed the best, having an  $R^2$  of 0.6 that tested significant in ANOVA at 95% confidence. The residual plot, having a normal distribution, shows that the significance test can be trusted. There furthermore appears to be no heteroscedacity in the regression, meaning that the error about the estimate remains constant throughout. Model 3 also had the lowest RMSE at  $0.55\text{mg/m}^3$ , and the lowest CV at 0.13.

The next best model, model 2, was based on observations of the spectral profile and had an  $R^2$  of only 0.18. Model 1, which was based on spectral values optimized for the Azov Sea in Russia, performed worst with an  $R^2$  of 0.08. Both models 1 & 2 failed the ANOVA significance test at 95% confidence. The model performance statistics are shown in Table 1.

*Table 1: Comparison of model performances.*

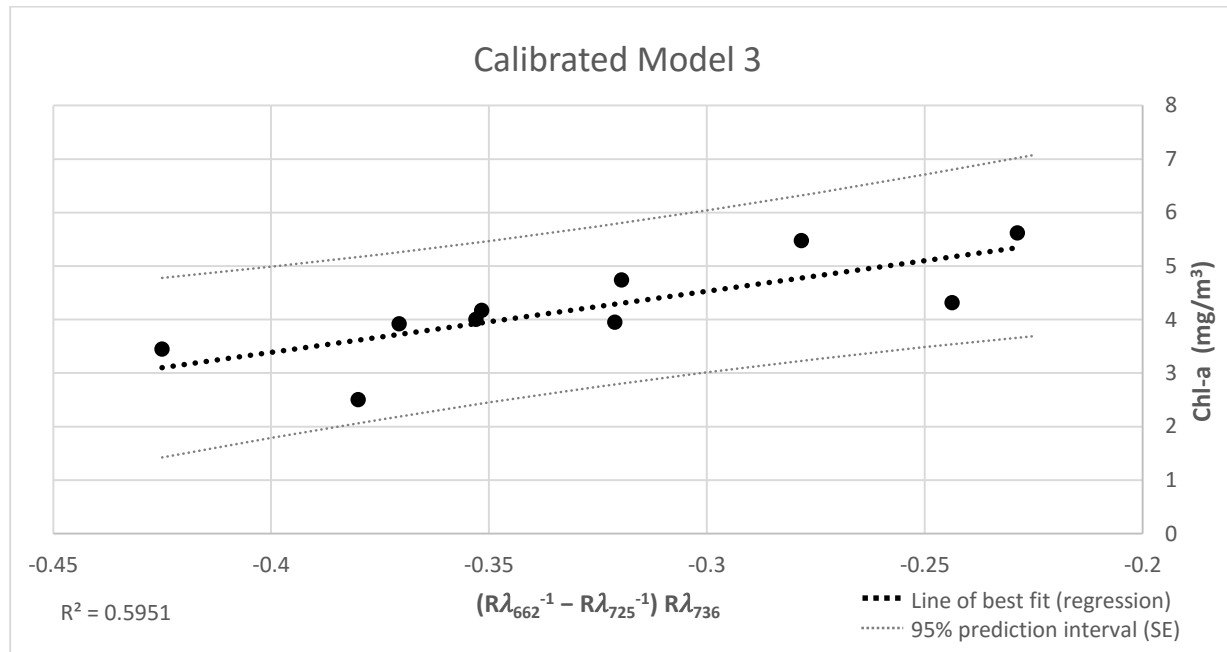
	$R^2$	ANOVA Significance (p)	RMSE	CV
<b>Model 3</b>	0.6	0.009*	0.55	0.13
<b>Model 2</b>	0.18	0.47	0.79	0.19
<b>Model 1</b>	0.08	0.43	0.83	0.2

\*p < 0.05 indicates the model is significant

The calibrated model 3 relating chl-a concentrations ( $\text{mg}/\text{m}^3$ ) in IRL to spectral properties of the HICO imagery is given by Equation 2. The model results extrapolated to estimate system wide IRL chl-a concentrations are mapped in Figure 4.

Equation 2: Calibrated Model 3

$$\text{Chl-a}(\text{mg}/\text{m}^3) = 11.406 \left( \frac{R\lambda_{736}}{R\lambda_{662}} - \frac{R\lambda_{736}}{R\lambda_{725}} \right) + 7.9497$$



The results of the optimization procedure confirm findings by Gitelson et al. (2011) that spectral bands should be narrow in order to estimate chl-a concentrations with a low RMSE. The relatively poor performance of the best model (model 3) when compared to other studies may be explained by data inconsistencies. In this study, in-situ measurements for the same date that imagery was collected were not available. Due to the transient nature of water, the

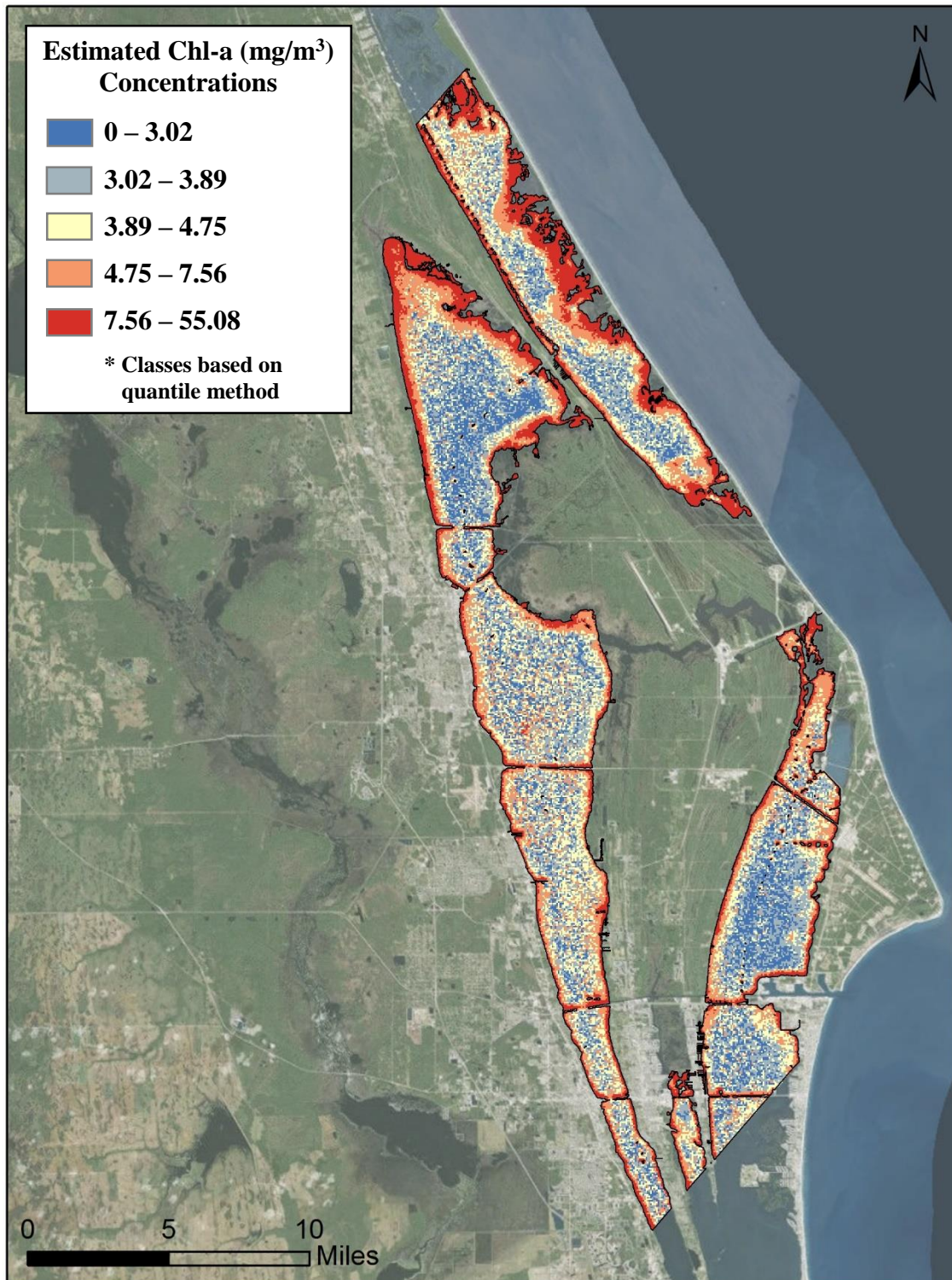


Figure 4: Chl-a concentrations ( $\text{mg}/\text{m}^3$ ) in IRL, mapped using model 3. Model 3 was obtained through optimizing wavelengths characterizing chl-a constituents in the lagoon, and calibration with observed in-situ chl-a concentrations. HICO imagery obtained from Oregon State University, chl-a measurements obtained from St. Johns River Water Management District. Service layer credits: Esri, DigitalGlobe, GeoEye, Earthstar, Geographics, CNES/Airbus DS, USDA, USGS, AEX, Getmapping, Aerogrid, IGN, IGP, Swisstopo, and the GIS User Community.

temporal difference between the calibration data may have greatly reduced quality of the model. Further reductions to model quality may be due to spatial differences between the in-situ measurements and the pixel location due to georeferencing errors. The pixel size of the obtained imagery itself is rather large at 88m, which results in pixels describing broadly the actual underlying distribution of chl-a concentrations within the pixels. The model optimization results may also be influenced by the validity of atmospheric correction performed on the original HICO imagery. Finally, the chl-a concentrations measured by SJRWMD are subject to errors and may slightly degrade model accuracy, although much less than the previously mentioned sources of error. The small number of available sample points also makes it difficult to conclusively test the reliability of the resulting model.

## Conclusion

Model 3 incorporating an optimization procedure vastly outperformed both model 1 transferred from the Azov Sea, and model 2 calibrated after selecting wavelengths through visual inspection of spectral signatures. Mapping of chl-a concentrations may benefit from improved data collection at higher resolution (of both the imagery and in-situ samples collected) with precise temporal and spatial overlap. However, these preliminary results indicate that it is possible to extract chl-a concentrations in IRL from hyperspectral imagery. The mapping procedure is efficient and results generally corroborate findings by others using similar methods (Bhatti, Schalles, Rundquist, Ramirez, & Nasu, 2010; Gitelson, Gao, Li, Berdnikov, & Saprygin, 2011; Kamerosky, Cho, & Morris, 2015; Olmanson, Brezonik, & Bauer, 2013; Shafique, Fulk, Autrey, & Flotemersch, 2003; Spectral Imaging Ltd.). However, the results of this study stress the need for improved data collection. The results indicate that it is not advisable to use models calibrated to specific water bodies on separate water bodies. Other researchers have also

observed that transfer of calibrated models from one site to another is subject to compatibility between study sites (Bhatti, Schalles, Rundquist, Ramirez, & Nasu, 2010). It is therefore advised that optimization procedures are adapted to all constituent mapping efforts, and that models are calibrated to the target water body.

The produced map suggest that chl-a concentrations are highest near the water's edge and lowest towards the center of the lagoon. There is, however, no visual correlation between anthropogenic influences and chl-a constituents. In fact, the least inhabited waters exhibit the highest chl-a concentrations. It is not clear whether extrapolations of the model beyond the interval of available observations can be trusted. The resulting map should therefore not be used to draw conclusions or test hypothesis. I am optimistic that future study with improved data will yield more reliable results in line with findings by other researchers who have used similar methods for mapping chl-a concentrations. In future studies, it may also be beneficial to incorporate uncertainties in the data to produce probability maps to aid interpretations of the mapped results.

## References

- Bhatti, A. M., Schalles, J., Rundquist, D., Ramirez, L., & Nasu, S. (2010). Application of Hyperspectral Remotely Sensed Data for Water Quality Monitoring: Accuracy and Limitation. *Accuracy 2010 Symposium*, (pp. 349-352). Leicester.
- Gitelson, A. A., Gao, B., Li, R., Berdnikov, S., & Saprygin, V. (2011). Estimation of Chlorophyll-a Concentration in Productive Turbid Waters Using A Hyperspectral Imager for the Coastal Ocean - the Azov Sea Case Study. *Environmental Research Letters*, 6, 1-6.
- Kamerosky, A., Cho, H. J., & Morris, L. (2015). Monitoring of the 2011 Super Algal Bloom in Indian River Lagoon, FL, USA, Using MERIS. *Remote Sensing*, 7, 1441-1460.
- Lapointe, B. E., Herren, L. W., Debortoli, D. D., & Vogel, M. a. (2015). Evidence of Sewage-driven Eutrophication and Harmful Algal Blooms in Flodida's Indian River Lagoon. *Harmful Algae*, 43, 82-102.
- Olmanson, L. G., Brezonik, P. L., & Bauer, M. E. (2013). Airborne Hyperspectral Remote Sensing To Assess Spatial Distribution of Water Quality Characteristics in Large Rivers: The Mississippi River and its Tributaries in MINnesota. *Remote Sensing of Environment*, 130, 254-265.
- Oregon State University. (2009). Retrieved 4 25, 2016, from HICO Hyperspectral Imager for the Coastal Ocean: <http://hico.coas.oregonstate.edu/>
- Shafique, N. A., Fulk, F., Autrey, B. C., & Flotemersch, J. (2003). Hyperspectral Remote Sensing of Water Quality Parameters for Large Rivers in the Ohia River Basin. *First Interagency Conf. on Research in the Watersheds*, (pp. 216-221).
- Spectral Imaging Ltd. (n.d.). Water Quality Monitoring. Oulu, Finland.
- St. Johns River Water Management District. (2016). *Water Quality*. Retrieved 4 25, 2016, from St. Johns River Water Management District: <http://www.sjrwmnd.com/hydrologicdata/waterquality/>